Journal of Materials Chemistry A

Accepted Manuscript

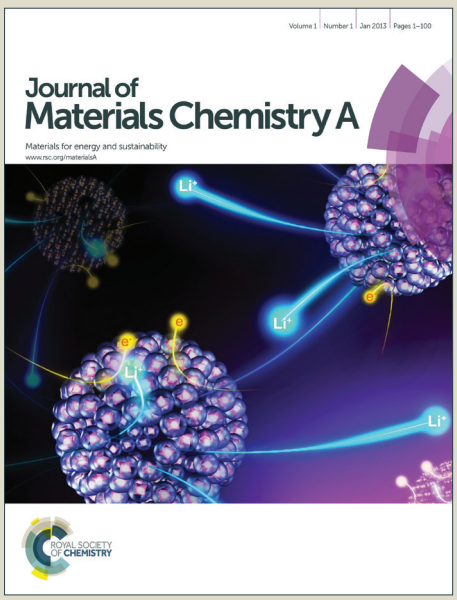

ROYAL SOCIETY OF CHEMISTRY

www.rsc.org/materialsA

Journal of Material Chemistry A RSCPublishing

Review

Developments of Furan and Benzodifuran Semiconductors for Organic Photovoltaics

Cite this: DOI: 10.1039/x0xx00000x

Peishen Huang, Jia Du, Michael C. Biewer* and Mihaela C. Stefan*

Received 00th January 2012,
Accepted 00th January 2012

DOI: 10.1039/x0xx00000x

www.rsc.org/

This review describes the developments of organic photovoltaic materials containing furan or benzo[1,2-*b*:4,5-*b'*]difuran (BDF) building blocks. Promising power conversion efficiencies above 6% have been achieved in the past two years for the BDF donor-acceptor polymers. Fundamentals of organic photovoltaics are briefly introduced at the beginning of this review. The uniqueness and advantages of BDF building block in semiconducting materials are discussed and compared with benzo[1,2-*b*:4,5-*b'*]dithiophene analogues.

Introduction

Organic semiconducting materials have drawn remarkable scientific and economic attention in the past three decades.[1-3] Tremendous progress has been achieved in electronic devices from organic materials due to their advantages such as low-cost, light-weight, solvent processability, and flexibility.[4-7]

In organic semiconducting compounds, the sp^2 hybridized atomic orbitals are used to form the σ-bonds with the neighbour atoms in the same plane. The p_z orbitals of adjacent atoms are perpendicular to the sp^2 plane and overlap to form the π-bonds. As a result, the electrons in the π-bonds are delocalized along the polymer backbone and further achieve certain opto-electronic properties. Poly(aniline) was first described to have color changing in different redox states,[8] which indicated the existence of resonance structures with variation of electron distributions in the molecular orbitals (MO).[9] In the 1970s, the studies on poly(acetylene) and its iodine-doped complexes boosted the area of organic conductive polymers.[10,11,12] Subsequently, poly(pyrrole),[13,14] poly(thiophene),[15,16,17] poly(*p*-phenylene vinylene),[18,19] and alkyl/alkoxy substituted aromatic rings[20,21] were developed. The alkyl/alkoxy side chains were covalently attached on the sp^2 hybridized atoms to increase the solubility of the π-conjugated polymers in organic solvents. Some examples of semiconducting polymers are shown in Figure 1.

Organic semiconducting materials can be divided into p-type and n-type depending on the relative energy levels of the HOMOs and LUMOs. Most donor-acceptor (D-A) alternating copolymers have relatively high HOMO levels and act as the p-type semiconductor in applications.[22,23] Fullerenes and their functionalized derivatives, like [6,6]-phenyl-C_{61}-butyric acid methyl ester ($PC_{61}BM$), are typical n-type semiconductors. Very few polymeric n-type materials have been reported.[24,25]

Recently, extensive research has been conducted on these un-doped π-conjugated polymers with intrinsic semiconducting properties.[26,27] The explored applications include organic field effect transistors (OFETs),[28,29] organic light emitting diodes (OLEDs),[30,31] and bulk heterojunction (BHJ) solar cells.[32,33]

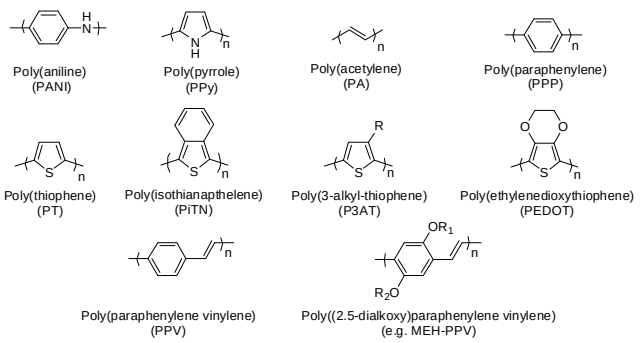

Figure 1. Structures of some semiconducting polymers used in organic electronics.

Sunlight, as a renewable energy source, can be directly converted to electrical power by photovoltaic devices. Of all the materials applied in photovoltaics, organic semiconducting materials have been developed rapidly with significant increase in performance.[34] The early organic solar cells were fabricated by using only p-type organic semiconductor as the active layer between the metallic electrodes (Figure 2a).[35] Before exposure to the light, the material is in the ground state.

The HOMO and those below it are filled with two electrons, while the LUMO and those above it are empty.[36] When the molecules absorb photons with energy higher than that of the band gap, neutral excited states can be generated.[37] In this case, an electron is promoted from the highest occupied molecular orbital (HOMO) to the lowest unoccupied molecular orbital (LUMO). A missing electron in a HOMO can be considered as a positive charge carrier, a

hole. Excitons, electron-hole pairs bound by coulombic force, are the precursors of free positive and negative charges in organic solar cells. In organic semiconductors, the coulombic attraction between electron and hole is relatively strong, resulting in the Frenkel exciton binding energy above 0.1 eV.[38] The high work function anode material and low work function cathode material are used to provide potential to split excitons generated in the active layer. However, this electric field between metal electrodes is not strong enough to split the Frenkel excitons. Poor performances with power conversion efficiencies (PCEs) below 0.5% were obtained in the single layer organic solar cells.[12,17,19] Later, a second layer of n-type semiconductor, phenyl-C_{61}-butyric acid methyl ester ($PC_{61}BM$) or phenyl-C_{71}-butyric acid methyl ester ($PC_{71}BM$), as the electron acceptor was introduced to generate an interface with the layer of p-type electron donor (Figure 2b). Both the p-type electron donor and the n-type electron acceptor play equally important rules in organic solar cells. The p-type electron donating polymers are the main light absorbers and the sources of the excitons. Fullerene as the electron accepting part in BHJ significantly increase the capture and splitting of the excitons as well as the transfer of electrons in the active layer.[39] Because of the differences of electron affinity and first ionization energy, strong electrostatic forces can be generated at the interface. This strong local electric field is useful for the splitting of excitons.[38] As a result, in this type of bilayer solar cell, PCEs were improved to above 1%.[40] However, within the short life time (< 1 ns) of Frenkel excitons in organic semiconductors, the excitons cannot diffuse to the interface beyond 20 nm.[38,41,42] In order to overcome this obstacle, bulk heterojunction (BHJ) solar cells were developed in 1990s (Figure 2c).[32] In a BHJ, p-type semiconducting polymers are mixed with $PC_{61}BM$ or $PC_{71}BM$, to generate phase separation in a form of a continuous and interpenetrating network. In the BHJ film, the contact area between polymer and $PC_{61/71}BM$ are significantly amplified. As a result, excitons can reach the phase boundaries more efficiently than the bilayer configuration.[39] The PCEs of organic solar cells have exceeded 8% with single-junction devices.[43,44,45] Lately, high PCE of 10.8% has been achieved by uncovering the temperature-dependent aggregation behavior of the donor polymers in BHJ.[46] Considering the different work function of metallic materials used for the electrons in OPV devices, normal and reversed device structures were developed. In the normal device structure, the high work function indium tin oxide is used as an anode. ITO is then covered by a layer of poly(3,4-ethylene dioxythiophene):polystyrene sulfonate (PEDOT:PSS) to enhance the hole transfer. The cathode is made by low work function metals such as silver, calcium or aluminum.

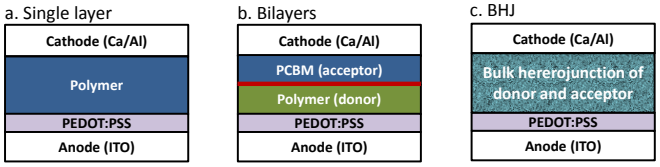

Figure 2. Development of the active layer in organic solar cells.

Figure 3 illustrates the mechanisms involved in the generation of light current in the BHJ active layer.[27,47,48,49] Four major steps are involved in the process of photocurrent generation. In the first step, excitons are generated in the active layer. Due to the high extinction coefficient of p-type polymer in the visible-IR range, compared with n-type fullerene derivatives, excitons are mainly formed in the p-type polymer domains.[50] In the second step, the generated excitons then diffuse to the interface between p-type polymer and n-type fullerene derivatives. In the third step, excitons are dissociated at the interface into free electrons and holes. Finally, holes move through the PEDOT: PSS to the ITO anode, while electrons are collected at the metal cathode.

The performance of the solar cell is described by the power conversion efficiency (PCE).[27] PCE is determined by the ratio of output power from the device and the input power from the light. The output power can be further expressed as the product of open-circuit voltage (V_{oc}), short-circuit current density (J_{sc}) and fill factor (FF) in equation 1. FF is defined in equation 2 and can be illustrated by Figure 4.[27]

$$PCE\ (\eta) = \frac{P_{out}}{P_{in}} = \frac{V_{oc} \times J_{sc}}{P_{in}} \times FF \quad (1)$$

$$FF = \frac{V_{max} \times J_{max}}{V_{oc} \times J_{sc}} \quad (2)$$

Energy levels of the HOMO and LUMO are crucial for the photon absorption and charge transfer in the BHJ.[51] Origin of V_{oc} was correlated strongly with the LUMO of fullerene acceptor and less sensitive to the Fermi level (E_F) of cathode metal.[51] Further study established a linear relation between V_{oc} and the oxidation potential of conjugated polymer shown in equation (3).[52]

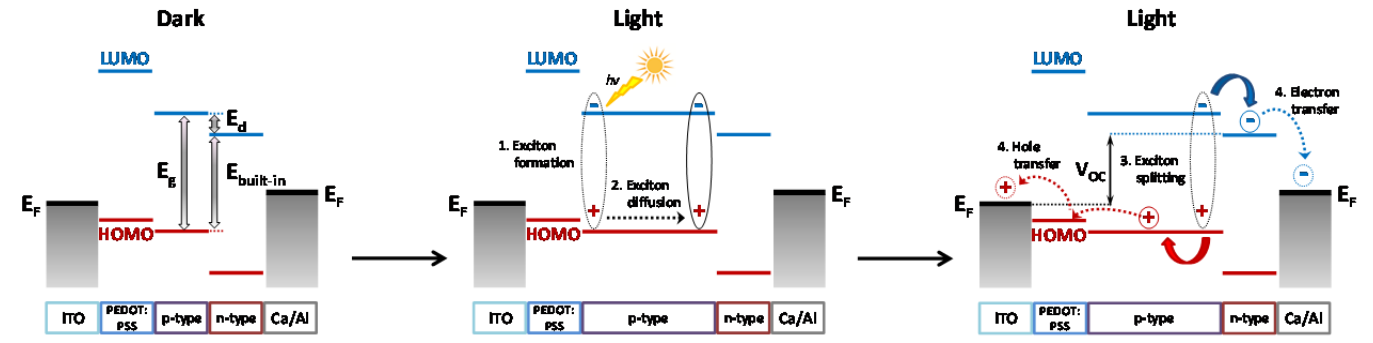

Figure 3. Schematic illustration of photocurrent generation under sunlight in the BHJ solar cell

The energy difference of HOMO of donor and LUMO of acceptor ($E_{built\text{-}in}$) is reduced by 0.3 V to be V_{oc}. The value of 0.3 V is an empirical factor which is related to the diode structure and working principle of the BHJ solar.[52] Relationship between V_{oc} and exciton binding energy was also studied.[53]

$$V_{OC} = \frac{|E_{HOMO}^{Donor}| - |E_{LUMO}^{PCBM}|}{e} - 0.3 \quad (3)$$

From equation (3), lower HOMO of the donor or higher LUMO of the acceptor could offer higher V_{oc}. However, these changes could simultaneously generate larger band gap (E_g) and narrower absorption width, which indicates loss of photons with lower energy from the sunlight. At the same time, the energy difference between LUMO levels of donor and acceptor (E_d) in BHJ needs to be larger than 0.3 eV to generate enough potential for splitting excitons.[54]

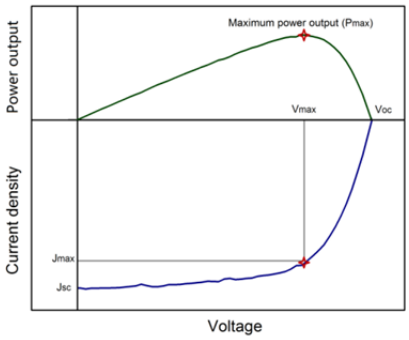

Figure 4. A typical current density (*J*) – Voltage (*V*) curve for an organic solar cell under illumination.

To minimize these conflicting requirements and optimize the synchronization of the parameters from a chemistry perspective, different electron sufficient aromatic units, the donors (D), and electron deficient units, the acceptors (A), are designed and synthesized for various alternating copolymers. Some fused aromatic rings are shown in Figure 5 as the examples of the donors (left) and acceptors (right).[55] The D-A alternating structure introduces a "push-pull" driving force to the π electrons to enhance the delocalization over the whole conjugated system. This orbital mixing effect between D and A can lead to a relatively higher lying HOMO and lower lying LUMO for the newly formed MOs, shown in Figure 6.[27] As a result, the band gap values can be reduced to further benefit the photon capture. At the same time, different combination of donor and acceptor moieties will be able to generate different absolute levels of HOMO and LUMO levels to balance the requirements for charge transfer.

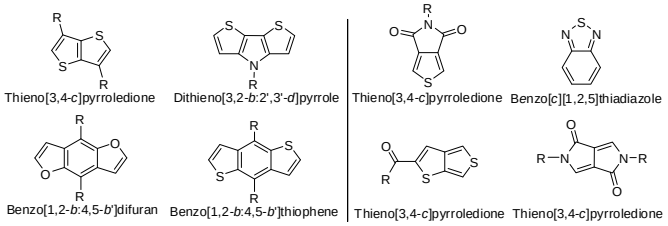

Figure 5. Examples of fused aromatic rings as repeating units in semiconducting polymers.

J_{sc} and FF are mainly determined by the nature and the purity as well as the morphology of the materials in the solid state. The increasing length of backbones, bulky alkyl side chains, and unsymmetrical monomer structures can introduce a high degree of conformational disorder and make many of the π-conjugated polymers amorphous.[56] Thus, the electronic benefit of increased conjugation length is restricted after a certain number of repeating units.[57] In BHJ, molecules are the subunits for the charge transfer.[36] As a result, various device fabrication techniques such as thermal annealing,[58,59] solvent annealing,[60] the use of small molecule additives in the active layer[61,62] and surface treatments[63,64] have been developed to optimize the interaction of polymer chains with the environment (other polymer chains and PCBM) in molecular level from an engineering standpoint.

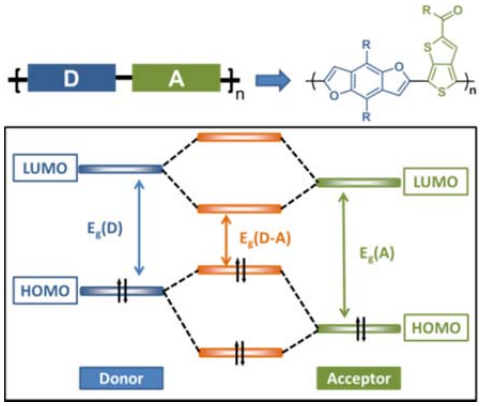

Figure 6. Orbital mixing of electron donating and withdrawing units.

Recent Benzodithiophene Polymers in OPV

Benzo[1,2-*b*:4,5-*b'*]dithiophene (BDT) is considered to be one of the most productive electron donating structures among various π-conjugated monomers designed and synthesized for donor-acceptor semiconducting copolymers. Symmetric and planar conjugated structures of BDT can help to improve the π-π stacking of the polymer backbone and hence increase the charge carrier mobility. Different types of substituents can be covalently connected on the 4 and 8 positions of BDT to optimize the solubility and energy levels of the materials.[23, 65-67] The first report of BDT semiconducting copolymers in BHJ solar cells was from Hou et al in 2008.[68] The BDT copolymer alternated with thiophene (**P1**) offered PCE of 1.6% (Figure 7, Table 1) which was the best performance among the eight different structures in this work. Different side chains have been attached to the BDT building block, including bithiophene,[69, 70] ethynyl,[71-76] phenylethynyl,[77-82] and alkylphenyl.[43,83] PCEs obtained from these diverse structures are located in a range of 1% to 8%. Recently, the D-A copolymers with BDT building blocks have reached PCEs above 9% in OPV application.[84]

Table 1. Optoelectronic and photovoltaic data of BDT D-A copolymers with alkyl and alkoxy substituents (**P1**, **P2** and **P3a-e**)

	HOMO (eV)	LUMO (eV)	E_{gopt} (eV)	[P]: PCBM	V_{oc} (V)	J_{sc} (mA/cm^2)	FF	PCE (%)
P1	-5.05	-2.69	2.36	1:1[a]	0.75	3.78	0.56	1.60[68]
P2	-5.36	-3.05	2.02	1:2[a]	0.78	13.30	0.70	7.30[85, 86]
P3a	-	-	-	1: 1.5[b]	0.96	10.80	0.68	6.90[87, 88]
				1: 1.5[bc]	0.93	12.50	0.65	7.30[87]
P3b	-	-	-	1: 1.5[b]	0.90	9.10	0.42	3.30[87]
				1: 1.5[bc]	0.93	8.30	0.53	3.80[87]
P3c	-	-	-	1: 1.5[b]	0.92	6.80	0.51	3.10[87]
				1: 1.5[bc]	0.89	6.50	0.45	2.50[87]
P3d	-	-	-	1: 1.5[b]	0.97	10.60	0.71	7.10[87]
				1: 1.5[bc]	0.97	12.60	0.70	8.30[87]
P3e	-	-	-	1: 1.5[b]	0.96	8.70	0.57	4.50[87]
				1: 1.5[bc]	0.96	11.10	0.62	6.30[87]

[a] $PC_{61}BM$ [b] $PC_{71}BM$ [c] 5% CN v/v additive

A D-A copolymer containing benzotriazole and BDT, **P2**, was first published by You et al.[89] In this work, the alkyl side chains were directly attached on the 4 and 8 positions of BDF (Figure 7). PCE of **P2** achieved 7.0% when trichlorobenzene was used as processing solvent.[85] Later on, the relationship between molecular weights of BDT and benzotriazole alternating copolymers and their OPV performances was established by the same research group. They found that **P2** with molecular weight around 40kDa gave reproducible PCE above 7%.[86]

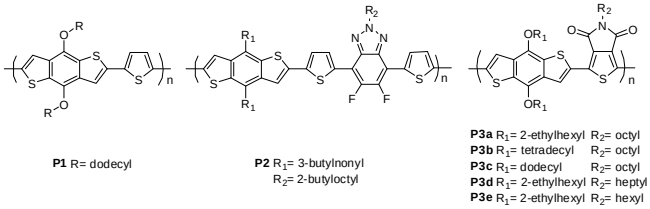

Figure 7. BDT D-A copolymers with alkyl and alkoxy substituents.

Cabanetos and coworkers focused on the effect of the linear side chains in BDT and thienopyrroledione based polymers **P3a-e**.[87] In their structures, on both of the electron donating moieties and electron accepting moieties, different combinations of branched and straight alkoxy chains (**P3a-e**) were tested (Figure 7). The linear alkyl chains on BDT would change the orientation of the polymer in thin film, which led to a decrease of the photovoltaic performance. With the chloronaphthalene (CN) additive, the combination of 2-ethylhexyl substituted BDT and heptyl substituted thienopyrroledione (**P3d**) gave the highest PCE of 8.5% (Table 1). Qu et al. studied the effect of different annealing conditions for polymer **P3a**.[88] PCE of 4.08% was obtained when the device was thermally annealed at 150 ^oC for 10 min. The PCE was increased up to 4.99% with solvent annealing using dichlorobenzene.

In 2011, Huo and coworkers optimized BDT structures by replacing the 2-ethylhexyloxy with 2-ethylhexylthienyl group (Figure 8).[90] **P4b** showed an increasing PCE from 6.43% to 7.59% with the incorporation of π-conjugated side chains. In comparison, **P4a** with the ester side chain on the thieno[3,4,*b*] thiophene acceptor performed lower PCE of 6.21% (Table 2).

Zhang et al. synthesized three different BDT unit with furan, thiophene and selenophene as side groups (Figure 8).[44] The dihedral angle between the BDT unit and conjugated side chains was also investigated. The BDT with furan as the side group had a dihedral angle of 34^o, which is smaller than the 60^o angle for the thiophene and selenophene analogs. As a result, polymer **P5a** showed smaller

Table 2. Optoelectronic and photovoltaic data of thienyl substituted BDT D-A copolymers

	HOMO (eV)	LUMO (eV)	E_{gopt} (eV)	[P]: PCBM[a]	V_{oc} (V)	J_{sc} (mA/cm^2)	FF	PCE (%)
P4a	-5.09	-3.22	1.58	1: 1.5[b]	0.68	14.59	0.63	6.21[90]
P4b	-5.11	-3.25	1.58	1: 1.5[b]	0.74	17.48	0.59	7.59[90]
P5a	-5.19	-3.64	1.55	1: 1.5[b]	0.69	11.77	0.65	5.28[44]
P5b	-5.24	-3.66	1.58	1: 1.5[b]	0.78	16.86	0.68	9.00[44]
P5c	-5.29	-3.71	1.58	1: 1.5[b]	0.81	16.57	0.66	8.78[44]
P6a	-5.30	-3.17	1.58	1: 1.5	0.78	15.41	0.61	7.38[91]
				1: 1.5[b]	0.77	14.99	0.64	7.42[91]
P6b	-5.18	-3.15	1.53	1: 1.5	0.74	14.67	0.64	7.42[91]
				1: 1.5[b]	0.73	15.17	0.64	7.10[91]
P6c	-5.41	-3.27	1.57	1: 1.5	0.84	15.32	0.65	8.42[91]
				1: 1.5[b]	0.83	15.49	0.59	7.58[91]
P6d	-5.33	-3.52	1.51	1: 1.5[b]	0.80	17.46	0.68	9.48[84]

[a] $PC_{71}BM$ [b] 3% DIO v/v additive

π-π stacking distance. However, **P5a** had the lowest J_{sc}. The furan side chains lifted the HOMO level of the material and generated low V_{oc}. Overall **P5a** had limited PCE of 5.28%. For polymer **P5b** and **P5c**, PCEs around 9.00% were obtained with J_{sc} above 16 mA cm^{-2} (Table 2).

Alkyl, alkoxy and alkylthio substituted thiophene side groups on BDT were developed by Cui et al (Figure 8).[91] The alkylthio substitution on thiophene were shown to lower the HOMO level of the BDT polymers and led to higher V_{oc}. Polymer **P6c** has V_{oc} of 0.84 V, which is higher than the 0.77 V and 0.73 V of polymer **P6a** and **P6b** respectively. A PCE of 8.42% was obtained by **P6c**, which is 1% higher than the other two (Table 2). Ye et al. continued working on the alkylthio substitution on thiophene side chains. The branched 2-ethylhexyl side chain was replaced by octyl straight chain (**P6d**).[84] The photovoltaic performance was further improved by increasing the PCE from 8.42% to 9.48%.

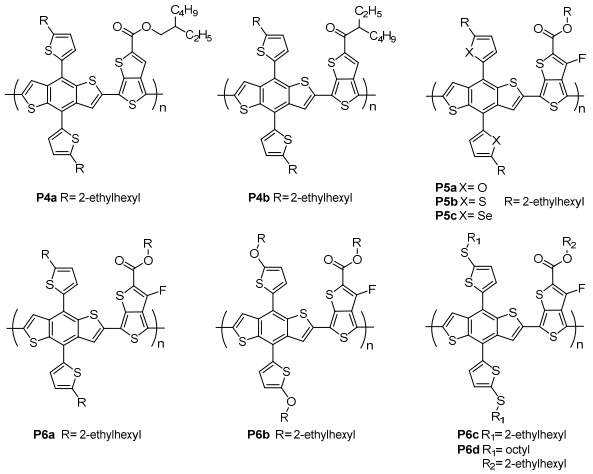

Figure 8. BDT donor with π-conjugated side chains and thieno-[3,4,*b*]thiophene acceptor in D-A copolymers.

Development of Furan and Benzodifuran Semiconductors in OPV

Due to increasing energy demands and environmental impact concern, harvesting clean solar energy has become increasingly important.[92,48,93] Furan is an abundant product from renewable resources. The vegetable residues in food industry and agriculture are converted to furfural (furan-2-carboxaldehyde),[93] while metal catalyzed decarbonylation reactions can convert furfural to furan in large scale (Figure 9).[94]

While polymers containing thiophene, especially with benzodithiophene building blocks, are approaching PCEs of 10% in OPV applications,[84] renewable furan and its derivatives have begun to draw attention and interest for the application in organic semiconductors. Furan is a five-membered aromatic heterocycle containing one sp^2 hybridized oxygen atom instead of the sulfur atom in thiophene. Oxygen belongs to the sixth group in the periodic table same as sulfur. The more electronegative oxygen of furan affects the electronic and optoelectronic potentials, as well for its enlarged π-conjugated derivatives. Due to being in a lower row of the periodic table, oxygen has a considerably smaller covalent radius than sulfur, which could reduce the distance of π-π stacking for the charge carrier transfer. Based on Pauling's electronegativity scale,[95] oxygen has a electronegativity around 3.5. Sulfur has a relatively lower electronegativity at 2.5. In both furan and thiophene, the dipoles are directed towards the heteroatoms. At the same time, the furan has a dipole moment of 0.71D which is larger than the thiophene ring of 0.54D.[93] The aromatic building blocks with different heteroatoms generate various dipole moments in the structures and ultimately can make fine tuning of the HOMO/LUMO levels and band gaps possible.[55]

Poly(thieno[3,4,*b*]furan) (**P7**) is the one of the earliest semiconducting polymer that contains furan fused rings (Figure 10). Sotzing and coworkers prepared this low band gap homopolymer by performing electrochemical polymerization on an inert electrode.[96] This product showed low band gap of 1.04 eV and stable redox behavior. In the past five years, one of the most important developments in furan containing π-conjugated materials is the application in BHJ solar cells. Most of the studies in this area are focused on the conjugated polymers with benzodifuran repeating units.

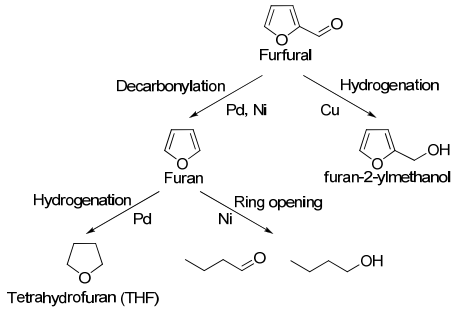

Figure 9. Decarbonylation of furfural over metal catalysts.

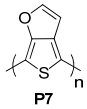

P7

Figure 10. Poly(thieno[3,4,*b*]furan) prepared by electrochemical polymerization.

Table 3. Optoelectronic and photovoltaic data of ethynyl substituted BDF materials

	HOMO (eV)	LUMO (eV)	E_{gopt} (eV)	[P]: PCBM[a]	V_{oc} (V)	J_{sc} (mA/cm^2)	FF	PCE (%)
P8	-5.39	-3.32	2.07	1:1	0.83	3.71	0.39	1.19[97]
P9	-5.62	-3.90	1.72	1:1	0.75	4.00	0.34	1.05[78]
P10	-5.30	-3.26	2.04	1:2	0.81	2.24	0.44	0.79[97]
P11	-5.38	-3.21	2.17	1:4	0.50	3.45	0.33	0.57[98]
P12a	-5.06	-3.20	1.86	1:4	0.53	3.10	0.35	0.59[99]
P12b	-5.25	-3.61	1.64	1:4	0.45	3.74	0.31	0.53[99]
P12c	-5.18	-3.36	1.82	1:4	0.29	2.19	0.27	0.17[99]

[a] $PC_{61}BM$

Between 2010 and 2012, benzo[1,2-*b*:4,5-*b'*]difuran building blocks were combined with ethynyl segments in two different ways developed by the Biewer group and Decurtins group.

A series of unique benzo[1,2-*b*:4,5-*b'*]difuran polymers (Figure 11) were synthesized by Biewer and coworkers.[97] Phenylethynyl side chains extended the π-conjugation perpendicular to the polymer backbones. Meanwhile, the fused furan building blocks in BDF were fully incorporated in the polymer backbones. Semiconducting performances of BDF (**P8**) and BDT (**P9**) homopolymers as well as alternative copolymers (**P10**) were studied.[78, 97] In OFET measurements, hole mobilities were reached above 10^{-4} cm^2 V^{-1} s^{-1} for BDF homopolymers. The BDF homopolymer also offered the highest PCE of 1.19% in OPVs amongst the analogues (Table 3).

However, Decurtins et al. took a different strategy.[100] In their structures, sp hybridized carbons were directly incorporated in the polymer backbones, while fused furan rings were used to attach side chains. The furan moieties in BDF were substituted by nitrile and dialkyl amino groups. The benzene core is functionalized by iodine or ethynyl for Sonogashira coupling polymerization. With strong electron withdrawing carbonitrile substituents, the BDF units should be considered as the electron accepting moiety in these copolymers. A homopolymer (**P11**) and three alternating copolymers (**P12a-c**) were synthesized (Figure 11).[98, 99] The highest PCE of 0.59% was generated by the polymer alternated with single thiophene unit (Table 3). The homopolymer offered hole mobility of 10^{-5} cm^2 V^{-1} s^{-1} in OFET measurements. The diethynylbenzo[1,2-*b*:4,5-*b'*]difuran monomer was further modified to be single molecule redox switches for regulating the charge transfer on molecular scale.[101]

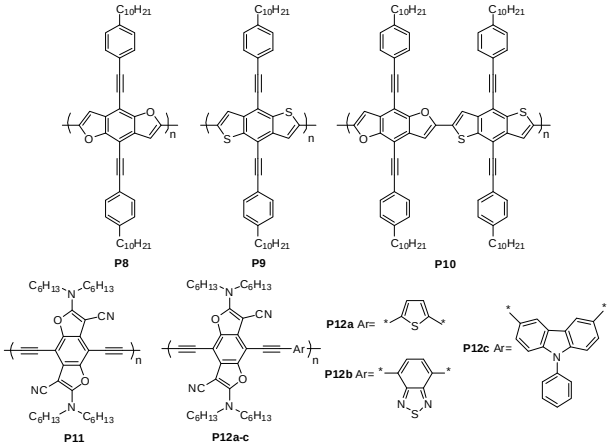

Figure 11. Structures of of ethynyl substituted BDF materials.

Benzodifuran monomers can be categorized by the different types of side chains attached on the fused benzene center. In the category of non-conjugated side chains, only 2-ethylhexyloxy and octyloxy were used on BDF.

Huo et al. synthesized a BDF monomer with 2-ethylhexyloxy side chains in 2012 (Figure 12).[102] This monomer was copolymerized with benzo[*c*][1,2,5]thiadiazole electron acceptor and alkyl thiophene spacer to form **P13** with Mw of 10kDa. A promising PCE of 5.01% was achieved by this pioneer of BDF materials (Table 4). At the same time, Li and coworkers made a series of three D-A copolymers with the same BDF electron donor with benzo[*c*][1,2,5] thiadiazole (**P14a**), benzotriazole (**P14b**) and benzo[*c*][1,2,5]oxadiazole (**P14c**) electron acceptors.[103] The polymer with alkoxy substituted benzo[*c*][1,2,5]thiadiazole repeating units offered the highest PCE of 4.45% in this series. Similar backbone structures of **P13** and **P14a** displayed the highest PCE values.

Table 4. Optoelectronic and photovoltaic data of alkoxy substituted BDF materials with benzo[*c*][1,2,5]thiadiazole, benzotriazole and benzo[*c*][1,2,5]oxadiazole electron acceptors

	HOMO (eV)	LUMO (eV)	E_{gopt} (eV)	[P]: PCBM[a]	V_{oc} (V)	J_{sc} (mA/cm^2)	FF	PCE[b] (%)
P13	-5.10	-3.24	1.60	1:1.5	0.78	11.77	0.55	5.01[102]
P14a	-5.11	-3.38	1.73	1:2	0.69	9.87	0.65	4.45[103]
P14b	-4.99	-3.06	1.93	1:2	0.44	4.92	0.58	1.24[103]
P14c	-5.19	-3.49	1.70	1:2	0.82	5.04	0.70	2.88[103]

[a] $PC_{71}BM$ [b] annealed at 90 °C for 10 min

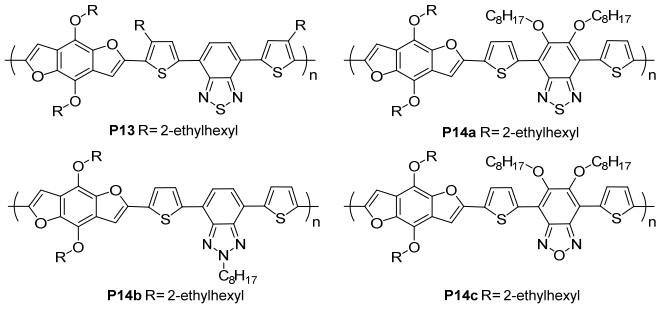

Figure 12. Structures of of alkoxy substituted BDF polyemers with benzo[*c*][1,2,5]thiadiazole, benzotriazole and benzo[*c*][1,2,5]oxadiazole electron acceptors.

Li's group reported BDF polymer structure with thieno[3,4,*b*]-thiophene acceptor (**P15**).[104] This polymer had a decent OPV performance with a PCE of 4.4% (Table 5). With the same 2-ethylhexyloxy substituted BDF monomer, Hou and coworkers performed further studies by changing the electron withdrawing groups on thieno[3,4,*b*]thiophene moiety (Figure 13).[105] Synthesis of various modified thieno[3,4,*b*]thiophene compounds were reported. The polymer **P16c** with fluorine on the thieno[3,4,*b*]thiophene units showed balanced V_{oc}, J_{sc} and improved PCE of 5.23%. The strong steric hindrance to the adjacent units from the cyano group was considered the reason for the low J_{sc} in **P16e**. By comparing **P15** and **P16a**, the BDF repeating units with octyl side chains showed slightly higher PCE than the one with 2-ethylhexyl branched side chains.

Table 5. Optoelectronic and photovoltaic data of alkoxy substituted BDF polymers with thieno[3,4,*b*]thiophene electron acceptors

	HOMO (eV)	LUMO (eV)	E_{gopt} (eV)	[P]: PCBM[a]	V_{oc} (V)	J_{sc} (mA/cm^2)	FF	PCE[b] (%)
P15	-5.27	-3.69	1.48	1:1.5	0.66	10.45	0.64	4.40[104]
P16a	-5.03	-3.63	1.53	1:1.5	0.54	13.13	0.60	4.26[105]
P16b	-5.07	-3.61	1.53	1:1.5	0.61	15.75	0.54	5.17[105]
P16c	-5.11	-3.60	1.52	1:1.5	0.63	13.88	0.60	5.23[105]
P16d	-5.25	-3.61	1.61	1:1.5	0.59	14.21	0.61	5.08[105]
P16e	-5.44	-3.70	1.60	1:1.5	0.82	4.78	0.47	1.85[105]

[a] $PC_{71}BM$ [b] 3% DIO v/v additive

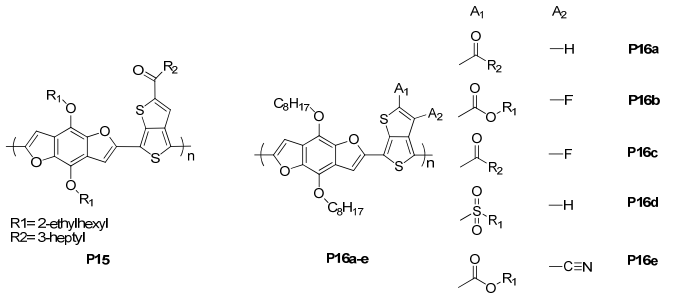

Figure 13. Structures of of ethynyl substituted BDF polymers.

In the work from Beaujuge and coworkers, the 2-ethylhexyloxy substituted BDF was polymerized with another well studied electron withdrawing monomer, thieno[3,4,*c*]pyrrole-4,6-dione (Figure 14).[106] This combination generated the highest V_{oc} of 0.97 among all the BDF structures that have been developed (Table 6). The high PCE of 6.9% (**P17c**) and the low PCE of 5.4% (**P17a**) are generated by the BDF polymers with the same backbone structure but different combination of alkoxy side chains on donor and acceptor moieties. The addition of chloronaphthalene (CN) additive decreased the performances of all the BDF polymers. However, their BDT polymer (**P18**) obtained increasing PCEs with CN additive. Grazing incidence X-ray scattering (GIXS) revealed the different intermolecular packing between the two analogous polymers **P17c** and **P18**. This morphological study further explains the different responses of **P17c** and **P18** to the CN additive in OPVs.

Table 6. Optoelectronic and photovoltaic data of alkoxy substituted BDF polymers with thieno[3,4,*c*]pyrrole-4,6-dione electron acceptors

	HOMO (eV)	LUMO (eV)	E_{gopt} (eV)	[P]: PCBM[a]	V_{oc} (V)	J_{sc} (mA/cm^2)	FF	PCE (%)
P17a	-	-	-	1:1.5	0.94	10.8	0.65	6.3[106]
				1:1.5[b]	0.95	9.8	0.60	5.4[106]
P17b	5.41[c]	3.44[c]	1.97[c]	1:1.5	0.97	11.2	0.68	6.9[106]
				1:1.5[b]	0.97	11.2	0.59	6.2[106]
P17c	-	-	-	1:1.5	0.93	11.3	0.69	6.9[106]
				1:1.5[b]	0.93	10.6	0.64	6.0[106]
P17d	-	-	-	1:1.5	0.94	9.1	0.67	5.6[106]
				1:1.5[b]	0.94	11.2	0.60	5.9[106]
P18	5.29[c]	3.44[c]	1.85[c]	1:1.5	0.94	11.1	0.66	5.6[106]
				1:1.5[b]	0.94	12.0	0.61	6.7[106]

[a] $PC_{71}BM$ [b] 5% CN v/v additive [c] estimated by photoelectron spectroscopy in air and UV-vis

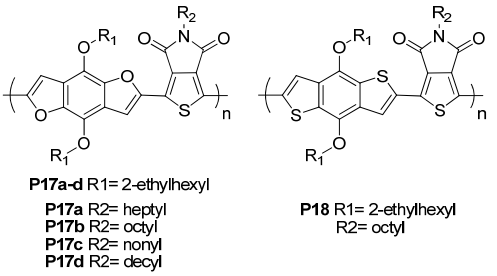

Figure 14. Structures of alkoxy substituted BDF polymers with thieno[3,4,*c*]pyrrole-4,6-dione electron acceptors.

In addition, thiophene and furan have been used to enhance the π-conjugation through the side chains. Li et al. synthesized a series of four BDT/BDF polymers with different combination of furan and thiophene building blocks in the electron donating monomers (Figure 15).[107] The BDF polymer with thiophene side chains (**P19c**) gave PCE of 4.00% without diiodooctane additive as the best one among the four polymers. However, this performance is still lower than that of **P13**, which has the same polymer structure but only alkoxy side chains on the BDF units. **P20** was synthesized recently by Zou and coworkers (Figure 15).[108] The thiophene conjugated side chains were attached on the BDF units, which is polymerized with the same electron acceptor as **P14a**. In this case, the π-conjugation through the thiophene side chains lowered the HOMO level in the polymer **P20** and increased the V_{oc} in OPV tests. **P20** with conjugated side chains offered more than 1% increase in PCE than its **P14a** analog (Table 4 and Table 7). In OFETs measurements, positive charge mobility of **P20** was obtained at 0.05 cm^2 V^{-1} s^{-1} with on/off ratio of 4.6 × 10^5. The photoresponse of the OFETs was also investigated and produced a photosensitivity (I_{light}/I_{dark}) of 1.2 × 10^5.[109]

Table 7. Optoelectronic and photovoltaic data of side chain conjugated BDF/BDT polymers with benzo[*c*][1,2,5]thiadiazole electron acceptors

	HOMO (eV)	LUMO (eV)	E_{gopt} (eV)	[P]: PCBM[a]	V_{oc} (V)	J_{sc} (mA/cm^2)	FF	PCE (%)
P19a	-5.26	-3.34	1.67	1:1	0.88	5.83	0.36	1.85[107]
P19b	-5.24	-3.24	1.70	1:1	0.85	8.41	0.40	2.88[107]
P19c	-5.08	-3.39	1.68	1:1	0.79	8.82	0.57	4.00[107]
				1.1[b]	0.73	9.94	0.61	4.42[107]
P19d	-5.11	-3.60	1.61	1:1	0.80	5.84	0.55	2.60[107]
P20	-5.21	-3.11	1.70	1:1.5	0.76	12.04	0.65	6.0[108]

[a] $PC_{71}BM$ [b] 3% DIO v/v additive

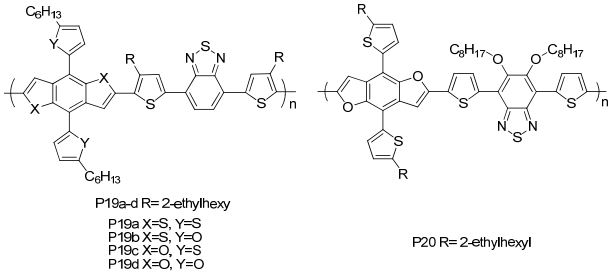

Figure 15. Structures of side chain conjugated BDF/BDT polymers with benzo[*c*][1,2,5] thiadiazole electron acceptors.

Hou et al. investigated the effects of conjugated and non-conjugated side chains on BDF with the fluorinated thieno[3,4,*b*]thiophene electron acceptor (Figure 16).[110] Conjugated thiophene side chains made the HOMO level of the **P22** around 0.2 eV lower than the **P21**, which does not have the π-conjugation in the side chains. With slight changes in J_{sc} and FF, **P22** gave a high PCE of 6.22% (Table 8).

Table 8. Optoelectronic and photovoltaic data of side chain conjugated BDF polymers with thieno[3,4,*b*]thiophene electron acceptors

	HOMO (eV)	LUMO (eV)	E_{gopt} (eV)	[P]: PCBM[a]	V_{oc} (V)	J_{sc} (mA/cm^2)	FF	PCE (%)
P21	-4.98	-3.18	1.51	1:1.5	0.63	12.51	0.57	4.52[102]
				1:1.5[b]	0.63	13.87	0.60	5.22[102]
P22	-5.21	-3.20	1.49	1:1.5	0.79	9.79	0.59	4.54[102]
				1:1.5[b]	0.78	13.04	0.62	6.26[102]

[a] $PC_{71}BM$ [b] 3% DIO v/v additive

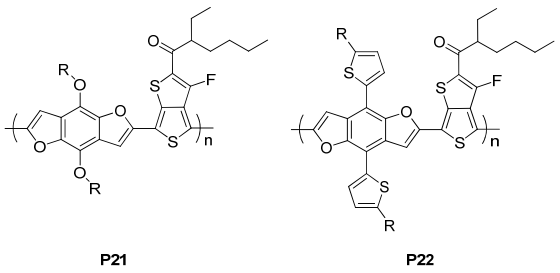

Figure 16. Structures of side chain conjugated BDF polymers with thieno[3,4,*b*]thiophene electron acceptors.

The investigation of the furan building block in the π-conjugated side chains has been continued with the study of furan spacers in the polymer backbone. It is a promising strategy to adjust the HOMO/LUMO levels and control the conformation of polymers by putting furan in different positions.

In the work of Yiu et al., the polymers with diketopyrrolopyrrole electron accepting moieties displayed improved solubility, nanostructure order and device performance when the thiophene co-mononor was reported with furan.[111] The switch from thiophene to furan did not impede the viable synthesis of diketopyrrolopyrrole in D-A-D co-monomer (Figure 17). PCE of 6.5% was achieved by relatively simple polymer structure without fused ring electron donor (**P23**).

Wang and coworkers synthesized four copolymers (**P24a-d**) with furan-diketopyrrolopyrrole comonomer and BDT donor shown in Figure 17. The incorporation of furan in both the side chains and the backbones (**P24d**) increased the PCE from 1.0% to 5.1%.[112] Similar strategy was applied on the benzo[*c*][1,2,5] oxadiazole acceptor by the same research group.[64] The polymer with the furan building blocks in both side chain of BDT units and polymer backbone (**P25c**) gave the highest PCE of 6.5% in the series (Table 9). The PCEs of **P25a-c** showed significant improvement of 130% - 170% after methanol or ethanol treatments of the dried active layers.

Table 9. Optoelectronic and photovoltaic data of D-A copolymers with furan side chains and spacers

	HOMO (eV)	LUMO (eV)	E_{gopt} (eV)	[P]: PCBM[a]	V_{oc} (V)	J_{sc} (mA/cm^2)	FF	PCE (%)
P23	-5.2c	-	1.4	1:3	0.65	14.8	0.64	6.5[111]
P24a	-5.05	-3.40	1.56	1:2[b]	0.62	3.87	0.40	1.0[112]
P24b	-5.15	-3,44	1.59	1:2[b]	0.63	8.78	0.53	2.9[112]
P24c	-5.16	-3.64	1.44	1:2[b]	0.69	10.46	0.49	3.5[112]
P24d	-5.24	-3.74	1.47	1:2[b]	0.72	12.64	0.57	5.1[112]
P25a	-5.34	-3.43	1.85	1:2[b,d]	0.83	10.6	0.65	5.6[64]
P25b	-5.44	-3.59	1.81	1:2[b,e]	0.86	9.1	0.59	4.5[64]
P25c	-5.40	-3.61	1.77	1:2[b,e]	0.83	12.7	0.62	6.5[64]

[a] $PC_{71}BM$ [b] 4% CN v/v additive [c] estimated by photoelectron spectroscopy in air [d] ethanol treatment on devices for 2 min [e] methanol treatment on devices for 2 min

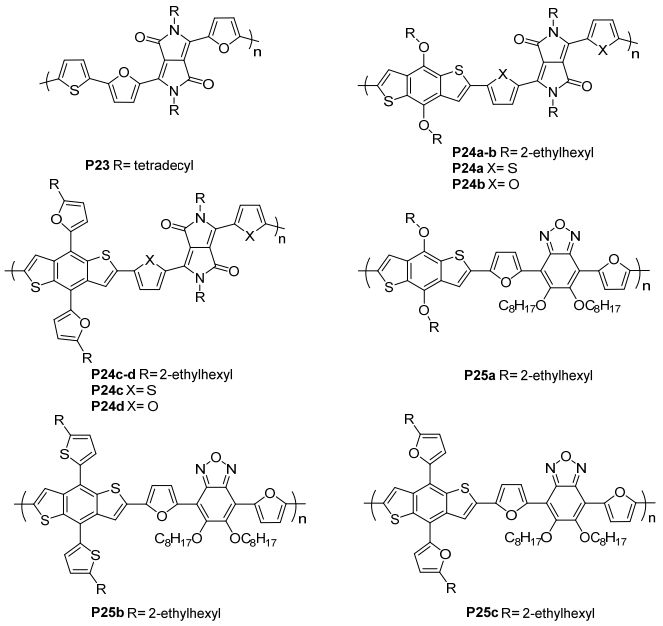

Figure 17. Structures of D-A copolymers with furan side chains and spacers.

Non-substituted benzodifuran donor units were published by Zhang et al in 2012.[113] In their work, benzo[1,2-*b*:5,4-*b'*]difuran (*syn*-BDF) and benzo[1,2-*b*:4,5-*b'*]difuran (*anti*-BDF) monomers were synthesized and incorporated into D-A copolymers with isoindigo electron deficient moieties (Figure 18). The syn-BDF polymer (**P26a**) showed a low HOMO of -5.63 eV. In UV-Vis, anti-BDF polymer (**P26b**) had a more red shifted absorption peak than the syn-BDF polymer, while the later one had stronger absorption coefficient around 475 nm. For **P26b**, 1% DIO additive in the active layer lowers the FF by 10%, but doubled the J_{sc}. PCE of 0.65% was achieved in both of the active layers with and without DIO. Higher PCE of 1.44% was obtained by **P26a** without DIO (Table 10).

Table 10. Optoelectronic and photovoltaic data of BDF semiconductors with unique structures

	HOMO (eV)	LUMO (eV)	E_{gopt} (eV)	[P]: PCBM[a]	V_{oc} (V)	J_{sc} (mA/cm^2)	FF	PCE (%)
P26a	-5.63	-3.90	1.73	1:2[a]	0.85	2.89	0.59	1.44[113]
P26b	-5.49	-3.85	1.64	1:2[a]	0.75	2.74	0.48	0.65[113]
P27	-5.55	-4.03	1.18	-	-	-	-	-
O1	-5.87	-3.79	2.10	bilayer[b]	0.66	4.01	0.40	1.18[92]

[a] $PC_{71}BM$ [b] $PC_{61}BM$

Benzodifuran-dione has been newly developed as an electron accepting moiety in D-A copolymers by Qiu and coworkers (Figure 18).[114] In this case, alkyl substituted bithiophene was used as the electron donating moiety. The copolymer **P27** has a low band gap around 1.2 eV with deep LUMO level of -4.03 eV. The polymer displayed ambipolar charge transfer with hole mobility of 1.08 cm^2 V^{-1} s^{-1} and electron mobility of 0.30 cm^2 V^{-1} s^{-1}, respectively.

The only D-A oligomer (**O1**) with BDF building blocks for OPV application was published by Frère and coworkers.[92] A bithiophene electron donating group and an electron deficient pentafluorobenzene group are attached on the same furan fused ring in the BDF center (Figure 18). A deep HOMO level at -5.87 was observed for **O1**. The PCE of 1.18% obtained from bilayer solar cells shows a promising future of BDF D-A oligomers in OPV applications (Table 10).

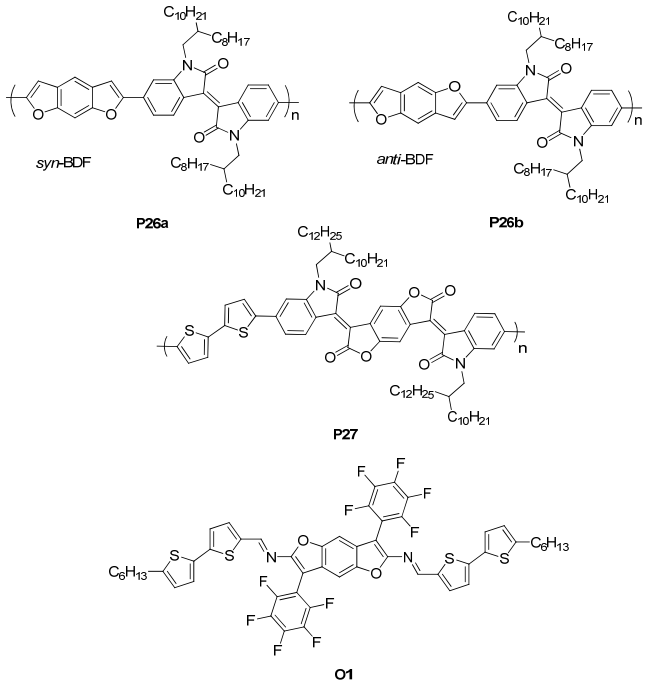

Figure 18. BDF semiconductors with unique structures.

The synthesis of furan oligomers was published by Thomas Kauffmann and Herbert Lexy in the early 1980s. Oxidative coupling

reactions with copper dichloride were used to synthesize all-α di/ter/quarter/octafuran (connected on 2 and 5 positions).[115,116]

The benzoxazole-terminated quater- and quinquafurans were synthesized by Kauffman and Moyna.[117] These functionalized furan oligomers were designed to be stable, efficient and fast fluorescence emitter. The furan-thiophene alternating oligomers, oligo(thienyl furan)s, were developed by Komatsu et. al in 2005.[118] The hole mobility of oligo(thienylfuran)s with different chain length were located in the range of 10^{-2}-10^{-4} cm^2 V^{-1} s^{-1} in OFET measurements.[119]

In 2010, Bendikov and coworkers synthesized α-oligofurans which have 5 to 9 repeating furan via Stille coupling of mono or difunctionalized bifuran and terfuran.[120] The products showed reasonable solubility up to eight repeating units. All of the α-oligofurans displayed better solubility in heptane than the α-oligothiophenes, as well as higher HOMO levels in CV when the number of repeating units is the same. The single crystal XRD data demonstrated a tighter herringbone packing with significant shorter distance between planes in α-hexafuran than α-hexathiophene. Strong red shifts could be observed in the UV-Vis spectra of the α-oligofurans with the increasing repeating units. However, a combination of light and heat could accelerate the decomposition of α-oligofurans. Bendikov and Perepichka then used the α-hexa/octafurans as p-type semiconductors in OFET. Hole mobilities of 0.05-0.07 cm^2 V^{-1} s^{-1} are very close to the thiophene analogs.[121]

Later in 2012, β-oligofurans (connected on the 3 and 4 position) were made by Sherburn and coworker.[122] The synthesis was achieved by halogen-lithium exchange and Suzuki coupling. Single crystal XRD data showed different dihedral angle between two furan π planes changing with different chain length and adjacent atoms in β-oligofurans.

In the work of Henssler and Matzger, dimers containing thieno[3,2-*b*]furan were synthesized.[123] In this case, furan is part of the fused aromatic ring. Due to the asymmetrical structure of thieno[3,2-*b*]furan, three different dimers with different regioregularity can be achieved. Six different dimers (**O2a-e**) were synthesized in combination with thieno[3,2-*b*]thiophene (Figure 19). The relationship between the position of the oxygen atoms and the optoelectronic properties was established by UV-Vis, fluorescence spectroscopy and CV. Crystal π-π stacking motifs were observed for all the six dimers in the solid state.

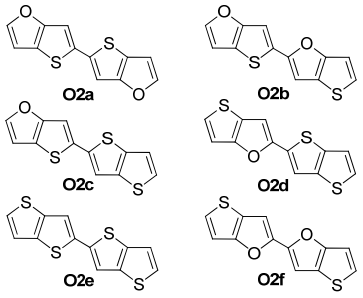

Figure 19. Six different dimers with thieno[3,2-*b*]furan and thieno[3,2-*b*]thiophene.

Conclusions

The research of organic semiconductors is still one of the hottest and most productive areas. It combines the knowledge and skills in organic chemistry and the practical viewpoints of engineering. Thiophene and its derivatives have made a solid progress with sunlight power conversion efficiency close to 10%. Furan is coming up with very promising performance in OPVs due to its economic advantages and structural specialties. BDF polymers have reached PCE above 6% in only 2-year study. Compared with BDT, the 2-D conjugated BDF polymer is less developed based on the relative low molecular weights and fewer modifications in the structures. In the area of organic small molecule OPVs, BDF structures are uncultivated. However, the methods developed in synthesis of the furan oligomers are viable for making more new furan containing π-conjugated materials.

Acknowledgements

NSF (Career DMR-0956116) and Welch Foundation (AT-1740) are gratefully acknowledged for the financial support (MCS). We thank the NSF-MRI grant (CHE-1126177) for supporting the Bruker Avance III 500 NMR (MCS).

Notes and references

Department of Chemistry, University of Texas at Dallas, Richardson, TX 75080, USA.
E-mail: biewerm@utdallas.edu; mihaela@utdallas.edu

1. A. G. Macdiarmid, *Angew. Chem. Int. Ed.*, 2001, **40**, 2581-2590.
2. A. J. Heeger, *Rev. Mod. Phys.*, 2001, **73**, 681-700.
3. H. Sirringhaus, *Nature Mater.*, 2003, **2**, 641-642.
4. Y. Liang, Z. Xu, J. Xia, S.-T. Tsai, Y. Wu, G. Li, C. Ray and L. Yu, *Adv. Mater.*, 2010, **22**, E135-E138.
5. A. Shah, P. Torres., R. Tscharner, N. Wyrsch and H. Keppner, *Science*, 1999, **285**, 692-698.
6. F. C. Krebs, S. A. Gevorgyan and J. Alstrup, *J. Mater. Chem.*, 2009, **19**, 5442-5451.
7. C. E. Small, S. Chen, J. Subbiah, C. M. Amb, S.-W. Tsang, T.-H. Lai, J. R. Reynolds and F. So, *Nature Photon.*, 2012, **6**, 115-120.
8. H. Letheby, *J. Chem. Soc.*, 1862, **15**, 161-163.
9. R. De Surville, M. Jozefowicz, L. T. Yu, J. Perichon and R. Buvet, *Electrochimica Acta*, 1968, **13**, 1451-1458.
10. H. Shirakawa, E. J. Louis, A. G. MacDiarmid, C. K. Chiang and A. J. Heeger, *J. Chem. Soc,. Chem. Commun.*, 1977, 578-580.
11. C. B. Gorman, E. J. Ginsburg and R. H. Grubbs, *J. Am. Chem. Soc.*, 1993, **115**, 1397-1409.
12. B. R. Weinberger, M. Akhtar and S. C. Gau, *Synthetic Met.*, 1982, **4**, 187-197.
13. A. F. Diaz, K. K. Kanazawa and G. P. Gardini, *J. Chem. Soc., Chem. Commun.*, 1979, 635-636.
14. A. F. Diaz, J. M. Vasquez Vallejo and A. M. Duran, *IBM J. Res. Develop.*, 1981, **25**, 42-50.
15. T. Yamamoto, K. Sanechika and A. Yamamoto, *J. Polym. Sci.: Polym. Lett. Ed.*, 1980, **18**, 9-12.
16. J. W-P. Lin and L. P. Dudek, *J. Polym. Sci.: Polym. Chem. Ed.* 1980, **18**, 2869-2873.
17. S. Glenis, G. Tourillon and F. Garnier, *Thin Solid Films*, 1986, **139**, 221-231.

18. J. H. Burroughes, D. D. C. Bradley, A. R. Brown, R. N. Marks, K. Mackay, R. H. Friend, P. L. Burns and A. B. Holmes, *Nature*, 1990, **347**, 539-541.
19. S. Karg, W. Riess, V. Dyakonov and M. Schwoerer, *Synthetic Met.*, 1993, **54**, 427-433.
20. R. D. McCullough and R. D. Lowe, *J. Chem. Soc., Chem. Commun.*, 1992, 70-72.
21. I. H. Campbell, D. L. Smith and J. P. Ferraris, *Appl. Phys. Lett.*, 1995, **66**, 3030-3032.
22. H. Usta, C. Risko, Z. Wang, H. Huang, M. K. Deliomeroglu, A. Zhukhovitskiy, A. Facchetti and T. J. Marks, *J. Am. Chem. Soc.*, 2009, **131**, 5586-5608.
23. R. S. Kularatne, H. D. Magurudeniya, P. Sista, M. C. Biewer and M. C. Stefan, *J. Polym. Sci. Part A: Polym. Chem.*, 2013, **51**, 743-768.
24. Y. Takeda, T. L. Andrew, J. M. Lobez, A. J. Mork and T. M. Swager, *Angew. Chem. Int. Ed.*, 2012, **51**, 9042-9046.
25. Y.-J. Hwang, N. M. Murari and S. A. Jenekhe, *Polym. Chem.*, 2013, **4**, 3187-3195.
26. M. P. Bhatt, H. D. Magurudeniya, E. A. Rainbolt, P. Huang, D. S. Dissanayake, M. C. Biewer and M. C. Stefan, *J. Nanosci. Nanotechnol.*, 2014, **14**, 1033-1050.
27. Y.-J. Cheng, S.-H. Yang and C.-S. Hsu, *Chem. Rev.*, 2009, **109**, 5868-5923.
28. H. Koezuka, A. Tsumura and T. Ando, *Synthetic Met.*, 1987, **18**, 699-704.
29. A. Facchetti, *Materials Today*, 2007, **10**, 28-37.
30. L. Duan, K. Xie and Y. Qiu, *Inf. Display-J. Soc. I.*, 2011, **19**, 453-461.
31. M. C. Gather, A. Köhnen, A. Falcou, H. Becker and K. Meerholz, *Adv. Funct. Mater.*, 2007, **17**, 191-200.
32. G. Yu, J. Gao, J. C. Hummelen, F. Wudl and A. J. Heeger, *Science*, 1995, **270**, 1789-1791.
33. G. Dennler, M. C. Scharber and C. J. Brabec, *Adv. Mater.*, 2009, **21**, 1323-1338.
34. F. C. Krebs, N. Espinosa, M. Hösel, R. R. Søndergaard and M. Jørgensen, *Adv. Mater.*, 2014, **26**, 29-39.
35. M. D. McGehee and M. A. Topinka, *Nature Mater.*, 2006, **5**, 675-676.
36. H. Bässler and A. Köhler, *Top. Curr. Chem.*, 2011, **312**, 1-65.
37. T. M. Clarke and J. R. Durrant, *Chem. Rev.*, 2010, **110**, 6736-6767.
38. A. A. Bakulin, A. Rao, V. G. Pavelyev, P. H. M. van Loosdrecht, M. S. Pshenichnikov, D. Niedzialek, J. Cornil, D. Beljonne and R. H. Friend, *Science*, 2012, **335**, 1340-1344.
39. A. Pivrikas, N. S. Sariciftci, G. Juška and R. Österbacka, *Prog. Photovolt.: Res. Appl.*, 2007, **15**, 677-696.
40. J. J. M. Halls, K. Pichler, R. H. Friend, S. C. Moratti and A. B. Holmes, *Appl. Phys. Lett.*, 1996, **68**, 3120-3122.
41. P. E. Shaw, A. Ruseckas and D. W. Samuel, *Adv. Mater.*, 2008, **20**, 3516-3520.
42. C. J. Bardeen, *Annu. Rev. Phys. Chem.*, 2014, **65**, 127-148.
43. M. Zhang, Y. Gu, X. Guo, F. Liu, S. Zhang, L. Huo, T. P. Russell and J. Hou, *Adv. Mater.*, 2013, **25**, 4944-4949.
44. S. Zhang, L. Ye, W. Zhao, D. Liu, H. Yao and J. Hou, *Macromolecules*, 2014, **47**, 4653-4659.
45. B. Zhao, Z. He, X. Cheng, D. Qin, M. Yun, M. Wang, X. Huang, J. Wu, H. Wu and Y. Cao, *J. Mater. Chem. C*, 2014, **2**, 5077-5082.
46. Y. Liu, J. Zhao, Z. Li, C. Mu, W. Ma, H. Hu, K. Jiang, H. Lin, H. Ade and H. Yan, *Nat. Commun.*, 2014, **5**, 5293.
47. F. C. Krebs, *Polymeric Solar Cells: Materials, Design, Manufacture*, DEStech Publications, 2010.
48. S.-S. Sun and N. S. Sariciftci, *Organic Photovoltaics-Mechanisms, Materials, and Devices*, CRCpress, 2005.
49. T. Kirchartz, J. Mattheis and U. Rau, *Phys. Rev. B*, 2008, **78**, 235320.
50. M. M. Wienk, J. M. Kroon, W. J. H. Verhees, J. Knol, J. C. Hummelen, P. A. van Hal and R. A. J. Janssen, *Angew. Chem. Int. ed.*, 2003, **42**, 3371-3375.
51. C. J. Brabec, A. Cravino, D. Meissner, N. S. Sariciftci, T. Fromherz, M. T. Rispens, L. Sanchez and J. C. Hummelen, *Adv. Funct. Mater*, 2001, **11**, 374-380.
52. M. C. Scharber, D. Mühlbacher, M. Koppe, P. Denk, C. Waldauf, A. J. Heeger and C. J. Brabec, *Adv. Mater.*, 2006, **18**, 789-794.
53. P. Yang, M. Yuan, D. F. Zeigler, S. E. Watkins, J. A. Lee and C. K. Luscombe, *J. Mater. Chem. C*, 2014, **2**, 3278-3284.
54. L. J. A. Koster, V. D. Mihailetchi and P. W. M. Blom, *Appl. Phys. Lett.*, 2006, **88**, 093511.
55. H. Zhou, L. Yang and W. You, *Macromolecules*, 2012, **45**, 607-632.
56. N. Tessler, Y. Preezant, N. Rappaport and Y. Roichman, *Adv. Mater.*, 2009, **21**, 2741-2761.
57. H. Sirringhaus, P. J. Brown, R. H. Friend, M. M. Nielsen, K. Bechgaard, B. M. W. Langeveld-Voss, A. J. H. Spiering, R. A. J. Janssen, E. W. Meijer, P. Herwig and D. M. de. Leeuw, *Nature*, 1999, **401**, 685-688.
58. E. Verploegen, R. Mondal, C. J. Bettinger, S. Sok, M. F. Toney and Z. Bao, *Adv. Funct. Mater.*, 2010, **20**, 3519-3529.
59. X. Yang and A. Uddin, *Renew. Sust. Energ. Rev.*, 2014, **30**, 324-336.
60. G. Li, Y. Yao, H. Yang, V. Shrotriya, G. Yang and Y. Yang, *Adv. Funct. Mater.*, 2007, **17**, 1636-1644.
61. A. K. K. Kyaw, D. H. Wang, C. Luo, Y. Cao, T.-Q. Nguyen, G. C. Bazan and A. J. Heeger, *Adv. Energy Mater.*, 2014, **4**, 11301469.
62. Z. Wang, F. Zhang, L. Li, Q. An, J. Wang and J. Zhang, *Appl. Surf. Sci.*, 2014, **305**, 221-226.
63. H. Zhou, Y. Zhang, J. Seifter, S. D. Collins, C. Luo, G. C. Bazan, T.-Q. Nguyen and A. J. Heeger, *Adv. Mater.*, 2013, **25**, 1646-1652.
64. Y. Wang, Y. Liu, S. Chen, R. Peng and Z. Ge, *Chem. Mater.*, 2013, **25**, 3196-3204.
65. C. Gao, L. Wang, X. Li and H. Wang, *Polym. Chem.*, 2014, **5**, 5200-5210.
66. P. Sista, M. C. Biewer and M. C. Stefan, *Macromol. Rapid Comm.*, 2012, **33**, 9-20.
67. P. Sista, R. S. Kularatne, M. E. Mulholland, M. Wilson, N. Holmes, X. Zhou, P. C. Dastoor, W. Belcher, S. C. Rasmussen, M. C. Biewer and M. C. Stefan, *J. Polym. Sci. Part A: Polym. Chem.*, 2013, **51**, 2622-2630.
68. J. Hou, M.-H. Park, S. Zhang, Y. Yao, L.-M. Chen, J.-H. Li and Y. Yang, *Macromolecules*, 2008, **41**, 6012-6018.
69. R. S. Kularatne, P. Sista, H. Q. Nguyen, M. P. Bhatt, M. C. Biewer and M. C. Stefan, *Macromolecules*, 2012, **45**, 7855-7862.
70. R. S. Kularatne, F. J. Taenzler, H. D. Magurudeniya, J. Du, J. W. Murphy, E. E. Sheina, B. E. Gnade, M. C. Biewer and M. C. Stefan, *J. Mater. Chem. A*, 2013, **1**, 15535-15543.
71. Q. Shi, H. Fan, Y. Liu, W. Hu, Y. Li and X. Zhan, *Macromolecules*, 2011, **44**, 9173-9179.

72. J.-H. Kim, M. Lee, H. Yang and D.-H. Hwang, *J. Mater. Chem. A*, 2014, **2**, 6348.
73. J.-H. Kim, C. E. Song, H. U. Kim, A. C. Grimsdale, S.-J. Moon, W. S. Shin, S. K. Choi and D.-H. Hwang, *Chem. Mater.*, 2013, **25**, 2722-2732.
74. C. Bathula, C. E. Song, S. Badgujar, S.-J. Hong, I.-N. Kang, S.-J. Moon, J. Lee, S. Cho, H.-K. Shim and S. K. Lee, *J. Mater. Chem.*, 2012, **22**, 22224.
75. J.-H. Kim, H. U. Kim, J.-K. Lee, M.-J. Park, M. H. Hyun and D.-H. Hwang, *Synthetic Met.*, 2013, **179**, 18-26.
76. H. G. Kim, S. B. Jo, C. Shim, J. Lee, J. Shin, E. C. Cho, S.-G. Ihn, Y. S. Choi, Y. Kim and K. Cho, *J. Mater. Chem.*, 2012, **22**, 17709.
77. N. Hundt, K. Palaniappan, J. Servello, D. K. Dei, M. C. Stefan and M. C. Biewer, *Org. Lett.*, 2009, **11**, 4422-4425.
78. P. Sista, H. Nguyen, J. W. Murphy, J. Hao, D. K. Dei, K. Palaniappan, J. Servello, R. S. Kularatne, B. E. Gnade, B. Xue, P. C. Dastoor, M. C. Biewer and M. C. Stefan, *Macromolecules*, 2010, **43**, 8063-8070.
79. P. Sista, B. Xue, M. Wilson, N. Holmes, R. S. Kularatne, H. Nguyen, P. C. Dastoor, W. Belcher, K. Poole, B. G. Janesko, M. C. Biewer and M. C. Stefan, *Macromolecules*, 2012, **45**, 772-780.
80. P. Sista, M. Wilson, N. Holmes, R. S. Kularatne, E. A. Rainbolt, M. C. Biewer, P. C. Dastoor, W. Belcher, M. C. Stefan, *Sci. Adv. Mater.*, 2013, **5**, 512-518.
81. P. Sista, J. Hao, S. Elkassih, E. E. Sheina, M. C. Biewer, B. G. Janesko and M. C. Stefan, *J. Polym. Sci. Part A: Polym. Chem.* 2011, **49**, 4172-4179.
82. P. Sista, M. P. Bhatt, A. R. McCary, H. Nguyen, J. Hao, M. C. Biewer and M. C. Stefan, *J. Polym. Sci. Part A: Polym. Chem.*, 2011, **49**, 2292-2302.
83. M. Zhang, X. Guo, W. Ma, S. Zhang, L. Huo, H. Ade and J. Hou, *Adv. Mater.*, 2014, **26**, 2089-2095.
84. L. Ye, S. Zhang, W. Zhao, H. Yao and J. Hou, *Chem. Mater.*, 2014, **26**, 3603-3605.
85. J. R. Tumbleston, A. C. Stuart, E. Gann, W. You and H. Ade, *Adv. Funct. Mater.*, 2013, **23**, 3463-3470.
86. W. Li, L. Yang, J. R. Tumbleston, L. Yan, H. Ade and W. You, *Adv. Mater.*, 2014, **26**, 4456-4462.
87. C. Cabanetos, A. El Labban, J. A. Bartelt, J. D. Douglas, W. R. Mateker, J. M. J. Fréchet, M. D. McGehee and P. M. Beaujuge, *J. Am. Chem. Soc.*, 2013, **135**, 4656-4659.
88. B. Qu, D. Tian, Z. Cong, W. Wang, Z. An, C. Gao, Z. Gao, H. Yang, L. Zhang, L. Xiao, Z. Chen and Q. Gong, *J. Phys. Chem. C*, 2013, **117**, 3272-3278.
89. S. C. Price, A. C. Stuart, L. Yang, H. Zhou and W. You, *J. Am. Chem. Soc.*, 2011, **133**, 4625-4631.
90. L. Huo, S. Zhang, X. Guo, F. Xu, Y. Li and J. Hou, *Angew. Chem. Int. Ed*, 2011, **50**, 9697-9702.
91. C. Cui, W.-Y. Wong and Y. Li, *Energy. Environ. Sci.*, 2014, **7**, 2276-2284.
92. C. Moussalem, O. Segut, F. Gohier, M. Allain and P. Frère, *ACS Sustainable Chem. Eng.*, 2014, **2**, 1043-1048.
93. J. A. Joule and K. Mills, *Heterocyclic Chemistry*, Blackwell Publishing Ltd, 2010.
94. S. Sitthisa and D. E. Resasco, *Catal. Lett.*, 2011, **141**, 784-791.
95. G. L. Miessler and D. A. Tarr, *Inorganic Chemistry*, Prentice Hall, 2010.
96. A. Kumar, J. G. Bokria, Z. Buyukmumcu, T. Dey and G. A. Sotzing, *Macromolecules*, 2008, **41**, 7098-7108.
97. P. Sista, P. Huang, S. S. Gunathilake, M. P. Bhatt, R. S. Kularatne, M. C. Stefan and M. C. Biewer, *J. Polym. Sci. Part A: Polym. Chem.*, 2012, **50**, 4316-4324.
98. H. Li, P. Tang, Y. Zhao, S.-X. Liu, Y. Aeschi, L. Deng, J. Braun, B. Zhao, Y. Liu, S. Tan, W. Meier and S. Decurtins, *J. Polym. Sci. Part A: Polym. Chem.*, 2012, **50**, 2935-2943.
99. H. Li, P. Jiang, C. Yi, C. Li, S.-X. Liu, S. Tan, B. Zhao, J. r. Braun, W. Meier, T. Wandlowski and S. Decurtins, *Macromolecules*, 2010, **43**, 8058-8062.
100. C. Yi, C. Blum, M. Lehmann, S. Keller, S.-X. Liu, G. Frei, A. Neels, J. r. Hauser, S. Schürch and S. Decurtins, *J. Org. Chem.*, 2010, **75**, 3350-3357.
101. Z. Li, H. Li, S. Chen, T. Froehlich, C. Yi, C. Schönenberger, M. Calame, S. Decurtins, S.-X. Liu and E. Borguet, *J. Am. Chem. Soc.*, 2014, **136**, 8867-8870.
102. L. Huo, Y. Huang, B. Fan, X. Guo, Y. Jing, M. Zhang, Y. Li and J. Hou, *Chem. Commun.*, 2012, **48**, 3318-3320.
103. B. Liu, X. Chen, Y. Zou, L. Xiao, X. Xu, Y. He, L. Li and Y. Li, *Macromolecules*, 2012, **45**, 6898-6905.
104. B. Liu, X. Chen, Y. Zou, Y. He, L. Xiao, X. Xu, L. Li and Y. Li, *Polym. Chem.*, 2013, **4**, 470-476.
105. L. Huo, Z. Li, X. Guo, Y. Wu, M. Zhang, L. Ye, S. Zhang and J. Hou, *Polym. Chem.*, 2013, **4**, 3047-3056.
106. J. Warnan, C. Cabanetos, A. E. Labban, M. R. Hansen, C. Tassone, M. F. Toney and P. M. Beaujuge, *Adv. Mater.*, 2014, **26**, 4357-4362.
107. Y. Zhang, L. Gao, C. He, Q. Sun and Y. Li, *Polymer Chemistry*, 2013, **4**, 1474.
108. B. Liu, B. Qiu, X. Chen, L. Xiao, Y. Li, Y. He, L. Jiang and Y. Zou, *Polymer Chemistry*, 2014, **5**, 5002-5008.
109. W. Huang, B. Yang, J. Sun, B. Liu, J. Yang, Y. Zou, J. Xiong, C. Zhou and Y. Gao, *Org. Electron.*, 2014, **15**, 1050-1055.
110. L. Huo, L. Ye, Y. Wu, Z. Li, X. Guo, M. Zhang, S. Zhang and J. Hou, *Macromolecules*, 2012, **45**, 6923-6929.
111. A. T. Yiu, P. M. Beaujuge, O. P. Lee, C. H. Woo, M. F. Toney and J. M. J. Fréchet, *J. Am. Chem. Soc.*, 2012, **134**, 2180-2185.
112. Y. Wang, F. Yang, Y. Liu, R. Peng, S. Chen and Z. Ge, *Macromolecules*, 2013, **46**, 1368-1375.
113. C. Hu, Y. Fu, S. Li, Z. Xie and Q. Zhang, *Polymer Chemistry*, 2012, **3**, 2949-2955.
114. G. Zhang, P. Li, L. Tang, J. Ma, X. Wang, H. Lu, B. Kang, K. Cho and L. Qiu, *Chem. Commun.*, 2014, **50**, 3180-3183.
115. T. Kauffmann, *Angew. Chem. Int. Ed.*, 1979, **18**, 1-19.
116. T. Kauffmann and H. Lexy, *Chem. Ber.*, 1981, **114**, 3667-3673.
117. J. M. Kauffman and G. Moyna, *J. Heterocyclic Chem.*, 2002, **39**, 981-988.
118. Y. Miyata, T. Nishinaga and K. Komatsu, *J. Org. Chem.*, 2005, **70**, 1147-1153.
119. Y. Miyata, M. Terayama, T. Minari, T. Nishinaga, T. Nemoto, S. Isoda and K. Komatsu, *Chem. Asian J.*, 2007, **2**, 1492-1504.
120. O. Gidron, Y. Diskin-Posner and M. Bendikov, *J. Am. Chem. Soc.*, 2010, **132**, 2148-2150.
121. O. Gidron, A. Dadvand, Y. Sheynin, M. Bendikov and D. F. Perepichka, *Chem. Commun.*, 2011, **47**, 1976-1978.
122. T. Fallon, A. C. Willis, A. D. Rae, M. N. Paddon-Row and M. S. Sherburn, *Chem. Sci.*, 2012, **3**, 2133-2137.
123. J. T. Henssler and A. J. Matzger, *J. Org. Chem.*, 2012, **77**, 9298-9303.